



Deposited via The University of Sheffield.

White Rose Research Online URL for this paper:

<https://eprints.whiterose.ac.uk/id/eprint/99638/>

Version: Accepted Version

Article:

Mann, G., Ellis, A. and Twyman, L.J. (2016) Modifying the product distribution of a reaction within the controlled microenvironment of a colloidosome. *Macromolecules*, 49 (11). pp. 4031-4037. ISSN: 1520-5835

<https://doi.org/10.1021/acs.macromol.6b00723>

Reuse

Items deposited in White Rose Research Online are protected by copyright, with all rights reserved unless indicated otherwise. They may be downloaded and/or printed for private study, or other acts as permitted by national copyright laws. The publisher or other rights holders may allow further reproduction and re-use of the full text version. This is indicated by the licence information on the White Rose Research Online record for the item.

Takedown

If you consider content in White Rose Research Online to be in breach of UK law, please notify us by emailing eprints@whiterose.ac.uk including the URL of the record and the reason for the withdrawal request.

Modifying the product distribution of a reaction within the controlled microenvironment of a colloidosome

*G. Mann, A. Ellis and L. J. Twyman**

Department of Chemistry, University of Sheffield, Brook Hill, S2 7HF, UK

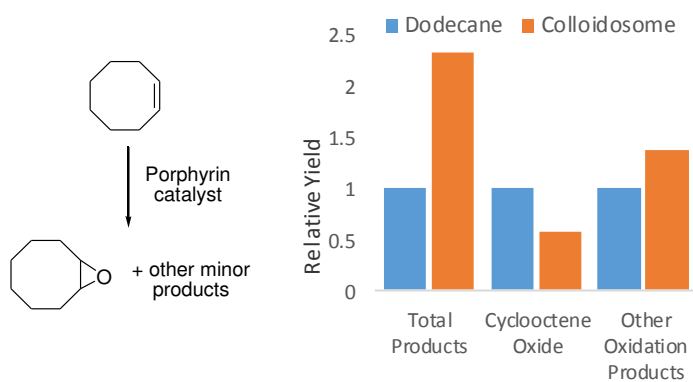
ABSTRACT

A water soluble colloidosome composed of PGMA-PS latex was used as a microcapsule to host a catalyzed oxidation reaction within its dodecane core. When compared to a control reaction a significant colloidosome effect was observed. Specifically, a 233% increase in the relative yield of all products was observed for the colloidosome reaction. Furthermore, when the product distributions were calculated it was evident that a switch in selectivity had taken place. These studies showed there is a significant reduction in the relative yield of the epoxide product compared to the remaining oxidation products. Additional control experiments confirmed that rate enhancements were not simply a result of concentration and that reactions were not occurring in the outer latex phase. As a consequence of these control experiments, we suggest that the colloidosome enhancement and shift in product distribution, comes about from differences in electronic environment at or close to the interface between the internal oil phase and the outer colloidal particles. This environment is able to stabilize any specific intermediates and or transition states leading to enhanced reactions for these products and higher relative yields.

For Table of Contents use only

Modifying the product distribution of a reaction within the controlled microenvironment of a colloidosome

*G. Mann, A. Ellis and L. J. Twyman**

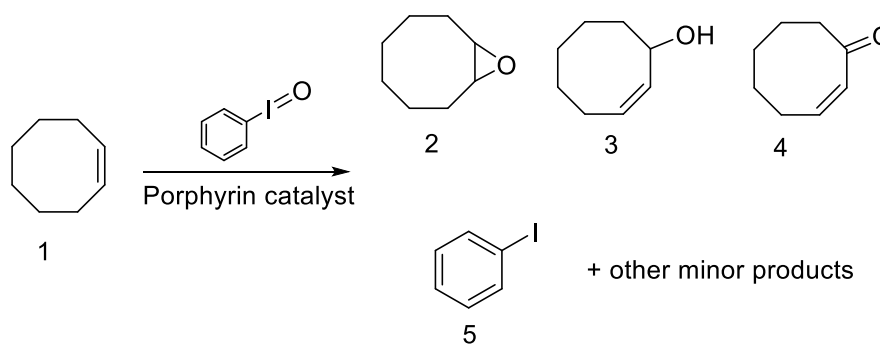


INTRODUCTION

Colloidal carriers including liposomes, ethosomes, lipospheres and nanoparticles,¹ are used in a range of areas. These include gene delivery, tumor targeting and oral medication.² A colloidosome is an alternative example of a vesicular system, offering promise in these areas.³ Colloidosome preparation involves stabilization at the interface of a Pickering emulsion,⁴ The resulting microcapsules are further stabilized by crosslinking to give robust microcapsules (colloidosomes).⁵ As a result of crosslinking, the microcapsule template is upheld when the internal oil phase is removed. With a colloidosome microcapsule, one has the capability to control numerous factors such as size, permeability, mechanical strength and compatibility. Depending on the polymer building block or particle type selected for synthesis, there is potential to manage the compatibility which facilitates the encapsulation of various entities, including biological material.^{3,6} For example, Lipase A from *Candida antarctica* (CalA), Lipase B from *Candida antarctica* (CalB) and benzaldehyde lyase from *Pseudomonas fluorescens* Biovar I (BAL) have been encapsulated and studied.⁷ The methods have been developed and the synthesis of crosslinked systems have also been reported. These microcapsules trap the encapsulated enzyme allowing them to withstand many purification cycles, whilst sustaining catalytic activity. The use of enzymes in confined spaces and their catalytic potential is an emerging field and a number of excellent reviews describe the current state of the research.⁸ Larger bacteria molecules have also been encapsulated,⁹ including *Lactobacillus crispatus*, which was encapsulated within a water-cored colloidosomes. Although they metabolized glucose at a slower rate, a larger number of bacteria remained viable even after exposure to HCl (pH 3.0) for 2 hours.¹⁰ In an effort to better control the stability and structure of colloidosome capsules, crosslinked or stabilized systems have also been developed. For instance, Duan *et al.* described the use of magnetic nanoparticles as stabilizers, giving rise to colloidosomes that could be influenced by an external magnetic field.¹¹ Another potential application for a colloidosome microcapsule, that is yet to be explored in detail, is catalysis. In this paper we report our initial proof of principle results describing how the micro-environment within a PGMA-PS latex colloidosome can affect the yield and product distribution of a multi-product reaction taking place within the oil phase of a water-soluble colloidosome. We also describe control experiments that confirm that rate enhancements are not simply a result of concentration. Additional controls also suggest that the reactions are taking place at or close to the interface between the internal oil phase and the outer colloidal particles.

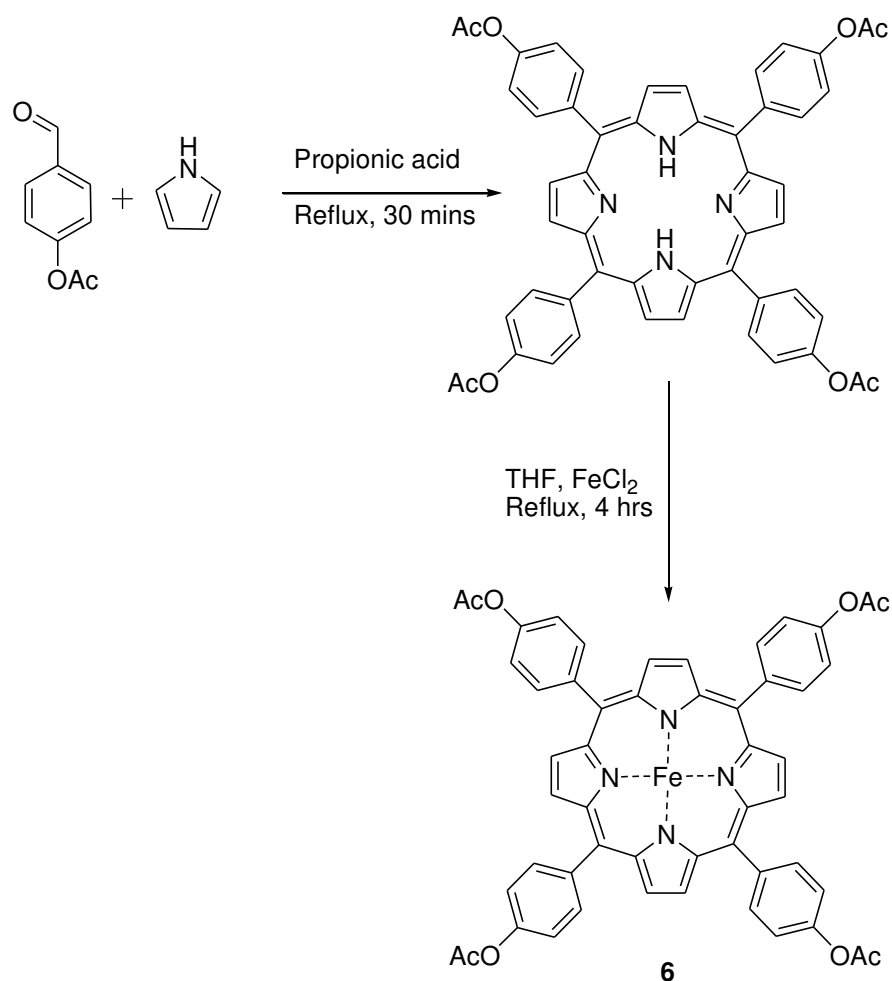
RESULTS AND DISCUSSION

In order to determine whether or not a colloidosome could modify a reaction carried out within its interior we first needed to identify a suitable reaction that would work to a measurable extent in dodecane. Furthermore, any reaction should also be capable of generating a number of products in measurable proportions. In recent related work we have studied the catalytic properties of porphyrin cored hyperbranched polymers. The specific reaction utilized an iron porphyrin that could catalyze the oxidation of cyclooctene **1**, with iodosylbenzene as the oxygen source.¹² The reaction generates the epoxide **2** and a number of other oxidation products **3**, **4** and **5**, some of which are shown in Scheme 1. In this respect it satisfies the proof of principle criteria required for this study.



Scheme 1; Catalytic epoxidation of cyclooctene indicating the mixture of products obtained. The yield of **2** was determined using GC. The yield of **5** was also determined using GC. The yield of all remaining oxidation products (**3**, **4** and other minor products) was calculated by subtracting the yield of **2** from **5**.

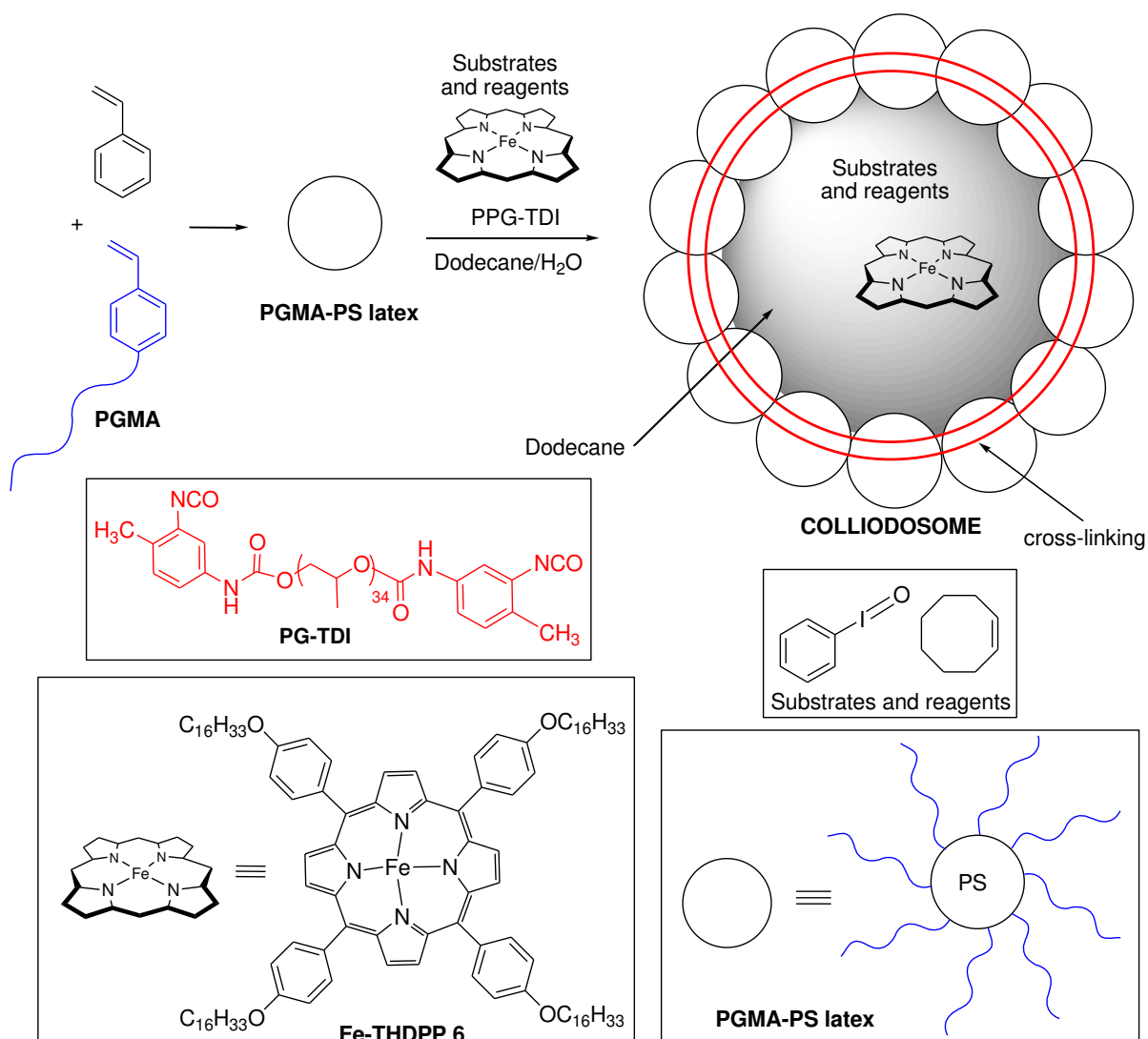
For our colloidosome study the porphyrin catalyst would need to be soluble within the dodecane core. As such the hexadecane functionalized porphyrin, 5, 10, 15, 20-Tetra(4-hexadecyloxyphenyl)porphyrin **6** (Fe-THDPP), was synthesized by reacting 4-(hexadecyloxy) benzaldehyde with pyrrole in the presence of catalytic boron trifluoride diethyl etherate, followed by oxidation using 2, 3-dichloro-5, 6-dicyano-*p*-benzoquinone (DDQ).¹³ The final step involved insertion of the iron, which was achieved by reacting the porphyrin with iron(II) chloride and 2,6-lutidine in THF and after purification, dodecane soluble Fe-THDPP **6** was obtained in a reasonable 25% yield. Scheme 2.



Scheme 2: Synthesis of Fe(III)-5, 10, 15, 20-tetrakis(4-acetoxyphenyl)-porphyrin **6** (Fe-THDPP).

Colloidosomes were assembled using PGMA-PS latex particles synthesized from a vinyl functionalized PGMA₅₀ macromonomer and styrene using an aqueous emulsification polymerisation.¹⁴ The resulting particles, dodecane and a cross linking agent (tolylene 2, 4-diisocyanate-terminated poly (propylene glycol) [PPG-TDI])¹⁵ were homogenized at room temperature with an aqueous phase containing 1% w/w of the latex particles. Two specific colloidosomes were constructed using the same general procedure. The first was a simple “empty” system that would act as a synthetic control, whilst a second colloidosome would contain the reagents, substrates, and the Fe-TDHPP **6** catalyst. The synthesis of the porphyrin encapsulated colloidosome is schematically represented in Scheme 3. After homogenization the initial “empty” colloidosomes were colorless, whereas the second system took on a red/brown color as a result of porphyrin encapsulation; Figure 1. In both cases the droplets were visualized by optical microscopy and sized using laser diffraction, with no detectable differences in droplet diameter observed between the two samples (50µm ±20 µm

in both cases). This provided confidence that the reagents, substrates, and catalyst (as well as any products formed) were not reacting with the cross-linker or affecting the colloidosome assembly process; Figure 2.



Scheme 3: Synthesis of the cross-linked colloidosome and the various components used in the catalytic reaction.

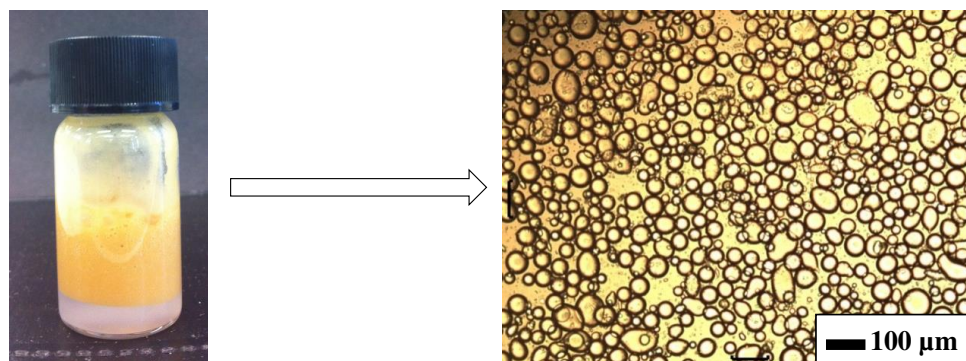


Figure 1: The porphyrin encapsulated colloidosome (left) and its optical microscopic image (right).

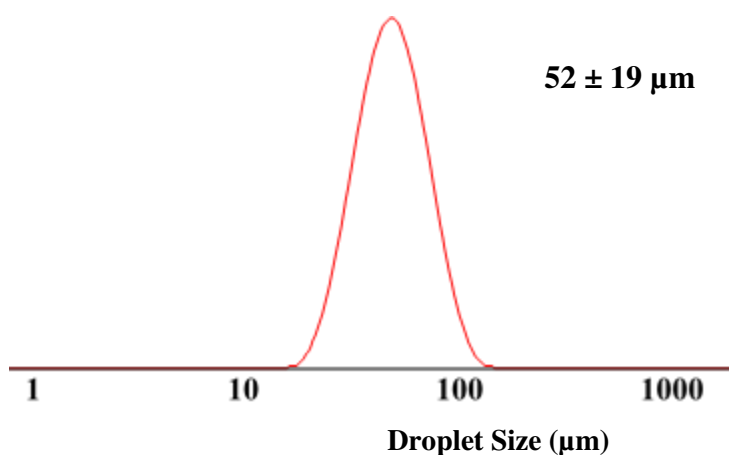


Figure 2: Droplet size/distribution recorded for the porphyrin colloidosome obtained using laser diffraction.

We now had all the molecules in place to start the catalytic experiments. Our first reaction would be a control designed to establish baseline yields of products from the Fe-THDPP **6** catalyzed reaction in dodecane. After work up and analysis by GC, a total yield of around 9% was determined for all oxidation products.¹⁶ Although this is relatively low, a number of products are formed and the yield is high enough for accurate measurement and therefore suitable for our “proof of principle” study. Analysis also indicated that the yield of epoxide **2** was lower than the total yield of all remaining oxidation products. All future yields would be compared *relative* to this control, non-colloidosome reaction. The next experiment would determine the relative yield of products obtained using the colloidosome encapsulated porphyrin catalyst; Fe-TDHPP **6**. Colloidosome systems were prepared such that the volume of dodecane and the amount of porphyrin, cycloctene and iododibenzene were the same as that used in the control reaction (i.e. concentrations of all species were identical for the control and colloidosome reactions). After 30 minutes the colloidosome suspension was extracted using dichloromethane and the organic layer collected and filtered into a GC vial for analysis. The results are displayed in Table 1 (1st column). The relative yield of oxidation products when the reagents and catalyst are encapsulated within the colloidosome was 21%, this is more than twice that measured for the background, non-colloidosome reaction and equates to a colloidosome enhancement of 233%. We were assuming that the reaction was taking place within the central dodecane component of the colloidosome. However, it is equally plausible to suggest that the reaction might be occurring within the polymeric structure, specifically within the polystyrene interior of the latex component. To test this possibility a second control experiment was carried out without the oil phase present. Specifically, a suspension of reagents, substrates, Fe-TDHPP **6** and latex particles was

suspended in bulk water and homogenised.¹⁷ The suspension was then agitated for 30 minutes before being extracted with dichloromethane and analyzed by GC. No products could be identified, indicating that the dodecane and (therefore) colloidosome are required for reaction. Furthermore, as the volume of dodecane and therefore the concentration of all species is identical for both sets of experiments, we can conclude that the enhancement is not due to increased concentration effects within the colloidosome. A further control was carried out to establish whether or not the colloidosome was able to effect the reaction on its own. As such, the reaction was repeated with the colloid and all reagents, but without the porphyrin catalyst. After extraction and careful analysis, a small amount of product was detected by GC, but this was small and within the error of the colloidosome experiments.

Having established a significant rate enhancement for all products, we set about to try and identify any colloidosome effect with respect to product selectivity. The oxidation reaction produces a major product, which is the epoxide **2**. Any effect of the colloidosome on product distribution can be determined by comparing the yield of epoxide **2** with the remaining oxidation products, using the by-product iodobenzene **5** as an internal standard, Scheme 1. The concentration of which be the same irrespective of the distributions of the oxidation products. The analysis was carried out and the results are shown below in Table 1. The data is normalized with respect to the yields obtained in the dodecane control reaction. When the same experiment was run using the colloidosome the total product yield increased, as described above. However, the distribution of products was not quite as expected. If we consider the product distributions recorded for the control reaction (carried out in dodecane), we can make a prediction for the yields we might expect using the colloidosome (i.e. assuming the colloidosome has no effect on product distribution). Specifically and based on a 233% enhancement, we can predict a relative yield of 0.63 for the epoxide **2** and 1.70 for the remaining oxidized products. When looking at the yields obtained in the colloidosome, we observe that the relative yield of epoxide **2** was 0.47. This is much lower than the expected relative yield of 0.63 and represents a *decreased* colloidosome effect. Conversely, when looking at the yield of all remaining oxidized products, we notice that the relative yield has risen to 1.86. This is higher than the predicted value (1.70) and represents an *increased* colloidosome effect. This led to the excess of remaining oxidized products increasing from 46% in the control/dodecane reaction, to 59% when the colloidosome was used. Or put more simply, although the total yield of products is much higher, the relative amount of cyclooctene oxide **2** is substantially reduced when the colloidosome was used. The data is

also shown graphically in Figure 3, using the yields relative to that obtained using dodecane (normalized and set to 1.0) for each data set.

	Total oxidation Products	Cyclooctene oxide	Remaining oxidation products	Excess of “Remaining oxidized products”
Relative yield in dodecane	1.00	0.27	0.73	46 %
Relative yield in colloidosome	2.33	0.47	1.86	59 %
Colloidosome effect ^(a)	233 %	174 %	255 %	/
Change in yield ^(b)	/	(-) 25 %	(+) 9 %	/
Shift in product distribution ^(c)			34%	

Table 1: Relative yields of cyclooctene oxide **2** and other oxidation products for the porphyrin catalyzed colloidosome and control reactions (Scheme 1). Data normalized for with respect to the total yield of products obtained using Fe-TDHPP **6** in dodecane. The data was calculated from an average set of at least six repeats. In all cases the maximum errors were no more than $\pm 15\%$. (a) Calculated using the % increase in yield between the dodecane and the colloidosome experiments. (b) The percentage increase or decrease in the predicted and actual yields (based on a colloidosome effect of 233 %). (c) Calculated by taking the differences in the “change of yield” for the cyclooctene and the “change in yield” for the remaining products.

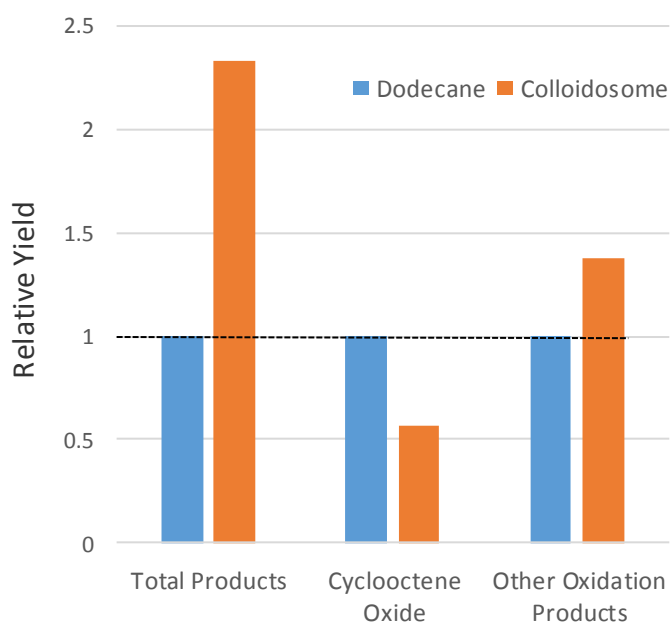
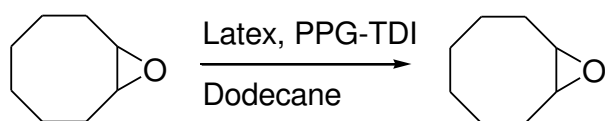


Figure 3: Relative yields for each set of products obtained from the control reaction in dodecane (blue) and colloidosome (red). For each data set (i.e. “total products”, cyclooctene oxide” or “other oxidation products”) the yields are normalized/set to 1.0 and displayed relative to those obtained in dodecane. Values below the line indicated a *negative* colloidosome effect and values above a *positive* colloidosome effect.

It could be argued that the large shift in the product distribution and reduced yield of epoxide **2**, may be due to a reaction between the nucleophilic components of the colloidosome and epoxide **2**, leading to the formation of ring opened structures that would lower the apparent yield of the epoxide **2** and increase the yield of the remaining/other oxidation products. To test this possibility an additional control experiment was carried out. The epoxide product **2** was added directly to a colloidosome preparation, Scheme 4. The mixture was left for 30 minutes and then extracted with dichloromethane, before being filtered into a GC vial and analyzed. The result indicated that $\pm 5\%$,¹⁸ all of the epoxide **2** remained after the experiment. Therefore, it is clear that epoxide **2** does not interact with the colloidosome and therefore, was not having a direct effect on the outcome of the oxidation reaction or product distribution.



Scheme 4: Control reaction to determine whether or not the cyclooctene product would react with the colloidosome. No reaction detected after 30 minutes.

Taking all of the data together, we can conclude that the enhanced yield and change in product distribution is a direct result of the reaction being carried out within the colloidosome. To understand how and where the reactions are taking place we need to consider the structure of the colloidosome in more detail, particularly with respect to the possible sites of reaction. The center of the colloidosome is essentially bulk dodecane, whilst the outer region is a latex. These are shown as regions A and B respectively in Figure 4. The control reactions, designed to test the validity of our experiments, could also be used to probe these two locations as possible sites for catalysis. For example, initial reactions were carried out using just dodecane as solvent, which provides the same environment as region A. However, substantially more product was obtained when the reaction was carried out using the colloidosome and identical concentrations of reactants/catalysts (with respect to the volume of dodecane used). Therefore, concentration arguments cannot be used to account for the observed colloidosome effects.

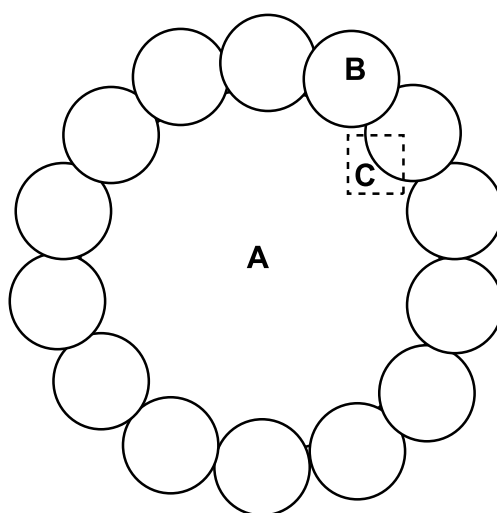
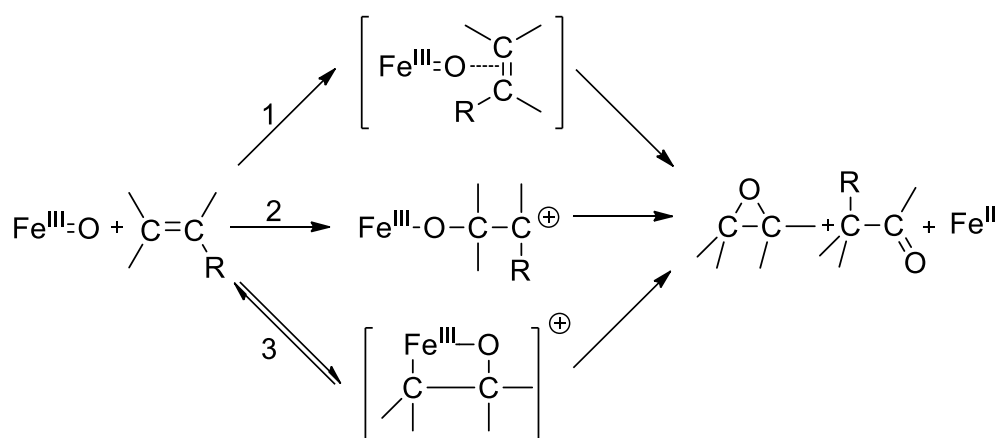


Figure 4: Possible locations within the colloidosome where oxidation could take place. (A) Within the dodecane oil core (B) within the PS particle, and (C) at the dodecane oil/PS particle interface.

The possibility of catalysis taking place in the latex region **B**, were also dismissed after studying the control using just the latex. In these experiments no products could be identified. As such the changes in yield(s) were entirely due to some aspect of the colloidosome structure. This leaves region **C**, the interface between the latex and the dodecane solvent. The oxidation reaction involves a number of pathways and intermediates, some of which are shown in Scheme 5.¹⁹ In all cases the relative proportion of products will be determined by the stability of these intermediates, or more importantly, the stability of any transition states. It is likely that the specific environment at the interface (between the

dodecane and the latex) will be able to affect the stability of these intermediates and transition states and favor an alternative reaction pathway. Therefore, an explanation for the change in product distribution could be a result of stabilization by some aspect/region of the colloidosome. For example, stabilization could occur through cation- π interactions²⁰ between the positively charged intermediate and the face of an electron rich aromatic ring present within the polystyrene component of the latex structure. Furthermore, if the reaction is taking place at the interface of the latex and the dodecane core, then the change in local dielectric environment could also account for the preferential stabilization of a different intermediates/transition states, resulting in a shift in product distribution. This is similar to the effect observed for reactions catalyzed at the polar surface/corona of micelles.²¹ In addition, it has been reported that local environments can affect the stability of particular spin states within the iron atom of the porphyrin catalyst. Changes in spin state are known to favor formation of alternative oxidation products.²²



Scheme 5 Possible pathways for porphyrin catalyzed epoxidation of an alkene. Pathway 1 represents the direct insertion of an oxygen atom, pathway 2 represents electrophilic addition followed by ring closure and pathway 3 represents the reversible formation of an electrocyclic metallooxetane followed by dissociation to generate the epoxide or other oxidation products.

CONCLUSIONS

In conclusion we have shown that a colloidosome can act as an effective micro-reactor capable of supporting a catalyzed reaction. Furthermore, we have revealed a colloidosome effect that leads to a 233% increase in the total yield of all products. A more significant result showed that a colloidosome could be used to effect the product distribution and outcome of a reaction where a number of products are possible. More specifically, we have

demonstrated that a dominant product can be “deselected” if the reaction is carried out within a colloidosome. The reason for these changes and improvements in yield comes from localized environmental effects generated by the colloidosome microcapsule, specifically at the dodecane/latex interface. More work is continuing to find and develop reactions with higher yields, as well as investigating the possibility of a two phase reaction, where product diffusion to bulk water may have a greater effect over product distributions and yields.

ACKNOWLEDGEMENTS

We would like to thank Professor S. P. Armes and Dr K. L. Thompson (University of Sheffield) for technical assistance and advice. We would also like to thank the EPSRC for funding (GM and AE).

EXPERIMENTAL

General experimental conditions

Solvents & Reagents. All chemicals and reagents were obtained from commercial sources (primarily Sigma-Aldrich) and were used without further purification unless otherwise stated. Bio-Beads® SX-1 was purchased from Bio-Rad Co. Dry solvents were dispensed from the Chemistry Department Grubbs System having thoroughly dried using molecular sieves.

NMR. All NMR samples were prepared using deuterated solvents supplied by Sigma Aldrich. ¹H NMR was performed at 250MHz and ¹³C NMR at 60MHz using a Bruker AC-250 with 5mm CH probe. In some cases ¹H NMR was performed at 400MHz using a Bruker AMX-400 with 5mm VSP multinuclear probe. Nucleus and frequency used accompanies all data in the text. **UV.** UV analysis was carried out using a Hitachi U-2010 spectrophotometer in wavelength mode.

IR. IR samples were recorded neat (without using Nujol or KBr) on a Perkin Elmer Spectrum RX I FT-IR spectrophotometer with integral DuraSampl IR-II.

Mass Spectrometry. Matrix assisted laser desorption ionization time of flight (MALDI-TOF) mass spectrometry was carried out using dihydroxybenzoic acid as the matrix on a Bruker Reflex III mass spectrometer with a mass range of 200-500,000 Da. **GPC.** Analytical GPC was conducted at room temperature using either a high molecular weight column setup consisting of 3x300mm PL gel 10um mixed-B, or a low molecular weight setup consisting of 2x600mm PL gel 5um (500Å). All samples were run using Fisher GPC grade THF stabilized with 0.025% BHT supplied to the columns by a Waters 515 HPLC Pump at 1.00 mlmin⁻¹.

Samples were prepared in THF and spike with toluene as a flow marker, before being injected through a 200ul sample loop with a Gilson 234 Auto Injector. Sample concentration was monitored using an Erma ERC-7512 refractive index detector and where relevant by UV using a Waters Millipore Lambda Max 481 LC Spectrophotometer. Data was analyzed using Polymer Labs proprietary software. **Gas Chromatography** was carried out using a PerkinElmer Autosystem XL Gas. Samples were carried out using H₂ gas flow using an Alltech AT1 non-polar column (length 30 meters, ID: 0.32 mm, Film Thickness 5.00 um). The injection temperature was 250°C, the oven temperature remained at 50°C for 5 minutes and then increased to 250°C over a 20 minute period. **Optical Microscopy** images were recorded using a Motic DMBA300 digital biological microscope equipped with a built-in camera and analyzed using Motic Images Plus 2.0 ML software. **Laser Diffraction** The volume-average droplet (D[4,3]) diameter was determined using a Malvern Mastersizer 2000 instrument equipped with a small volume Hydro 2000SM sample dispersion unit (ca. 50 ml), a He-Ne laser operating at 633 nm, and a solid-state blue laser operating at 466 nm. The stirring rate was adjusted to 1 000 rpm in order to avoid sedimentation of the emulsion during analysis. After each measurement, the cell was rinsed once with *n*-dodecane. The glass walls of the cell were carefully wiped to avoid cross-contamination and the laser was aligned centrally to the detector prior to data acquisition.

Synthesis

4-(hexadecyloxy) benzaldehyde. A mixture of bromohexadecane (5.50 g, 18.0 mmol), 4-hydroxybenzaldehyde (2.0 g, 16 mmol), potassium carbonate (2.72 g, 19.6 mmol) and a crystal of 18-crown-6 in anhydrous acetonitrile was refluxed for 3 days. The reaction mixture was concentrated in vacuum and the residue was dissolved in diethyl ether/water (1:1). The organic layer was washed three times with saturated aqueous sodium hydrogen carbonate, once with saturated brine solution and subsequently dried over magnesium sulphate. Evaporation of the solvent under vacuum affords the crude product. The product was purified by column chromatography and eluted with 20:1 petroleum ether 40-60: ethyl acetate. (R_f = 0.83, TLC was visualized using anisaldehyde staining). Yield 3.26 g, 57% ¹H NMR (CDCl₃, 400 MHz) δ_H 9.86 (s, 1H, R-CHO), 7.81 (d, 2H, phenylic *m*-CH, J=9.0), 6.97 (d, 2H, phenylic *o*-CH, J=9.0), 4.02 (t, 2H, OCH₂C₁₅H₃₁, J=7.0), 1.80 (m, 2H, OCH₂CH₂C₁₄H₂₉) 1.50-1.20 (bm, 26H, OCH₂CH₂C₁₄H₂₆CH₃), 0.87 (t, 3H, OC₁₅H₃₀CH₃, J=7.0); ¹³C NMR (CDCl₃, 400 MHz) δ_C 190.8, 164.3, 132.0, 129.7, 114.7, 68.4, 32.0, 29.6, 29.4, 26.0, 22.7, 14.2,) FTIR (cm⁻¹) 2916, 2848, 2738 (alkyl C-H stretch), 1683 (aldehyde C=O stretch), 1603, 1578, 1509,

1241 EA %: Carbon (Expected value: 79.71 %) Found: 79.42 % Hydrogen (Expected value: 11.05 %) Found: 11.38 % ES MS 347 (MH⁺) m.p. 42-44 °C.

5, 10, 15, 20-Tetra(4-hexadececycloxyphenyl)porphyrin Boron trifluoride diethyl etherate (37.30 μ l, 0.3 mmol) and a catalytic amount of anhydrous ethanol (1.95 mL, 30 mmol) were added to a solution of 4-hexadececycloxybenzaldehyde (1.05g, 3.0 mmol) and pyrrole (210.2 μ L, 3.0 mmol) in anhydrous dichloromethane (300 mL, 4.68 mol, 15.6 mol/L) at room temperature under argon. The reaction mixture was then stirred for 1hr in an inert gas stream at room temperature; 2, 3-dichloro-5, 6-dicyano-1,4 benzoquinone (619.0 mg, 2.7 mmol) was added and the mixture was stirred for another 1hr. The reaction products were separated by flash chromatography and eluted with chloroform. The target product was purified by column chromatography and eluted with chloroform. Yield 1.27 g, 25 % ¹H-NMR (CDCl₃, 400 MHz) δ _H 8.88 (s, 8H, pyrrolic β -H), 8.14 (d, 8H, phenylic *o*-CH J=8.0), 7.30 (d, 8H, phenylic *m*-CH J=8.5), 4.30 (t, 8H, OCH₂C₁₅H₃₁, J=6.0), 2.01 (bm, 8H, OCH₂CH₂C₁₄H₂₉) 1.72-1.23 (bm, 104H, OCH₂CH₂C₁₄H₂₆CH₃), 0.91 (t, 12H, OC₁₅H₃₀CH₃, J=6.5), -2.72 (s, 2H, NH), ¹³C-NMR (CDCl₃, 400 MHz) δ _C 159.0, 158.3, 144.1, 135.6, 134.6, 119.9, 114.3, 112.71, 100.9, 68.4, 32.0, 29.7, 29.4, 26.3, 22.7, 14.1 FTIR (cm⁻¹) 2918, 2850 (alkyl C-H stretch), 1509, 1241 EA %: Carbon (Expected value: 82.28 %) Found: 81.94 % Hydrogen (Expected value: 10.10 %) Found: 9.97 % Nitrogen (Expected value: 3.55 %) Found: 3.41 % MALDI TOFF MS 1575.4 (MH⁺) UV absorbance (CHCl₃) λ _{max} (nm) 423, 520, 557, 593, 651.

5.9.3 Synthesis of 5, 10, 15, 20-Tetra(4-hexadececycloxyphenyl)porphyrin Iron(III) complex 6
5, 10, 15, 20-Tetra(4-hexadececycloxyphenyl)porphyrin (50 mg, 3.17x10⁻² mmol) was dissolved in THF (25 mL) with Iron (II) chloride (80.4 mg, 0.634 mmol) and 2, 6-lutidine (9.2 μ L, 7.93x10⁻² mmol). The solution was warmed to 50 °C under reflux and stirred for 3 hours. Solvent was then removed via rotary evaporation and a 1:1 mix of chloroform and water was added to the flask. After vigorous shaking many insoluble impurities formed at the solvent interface and were removed via vacuum filtration. The organic layer was collected and solvent was removed via rotary evaporation and eluted through a silica column with 1:1 chloroform and methanol. Yield 25 mg, 50 % FTIR (cm⁻¹) 2917, 2849 (alkyl C-H stretch), 1511 (aromatic C=C stretch), 1242 (C-O) MS-MALDI 1631(MH⁺) UV absorbance (CHCl₃) λ _{max} (nm) 412, 573, 616.

Synthesis of Iodosylbenzene. 3M sodium hydroxide (15 mL) was added over 3 minutes to a beaker containing (Diacetoxyiodo) benzene (3.22 g, 0.01 mol) with vigorous stirring. The reaction was then left to stand for a period of 45 minutes. Distilled water (15 mL) was then added with continual stirring and the solid collected via vacuum filtration. The solid was then stirred in excess distilled water for a period of 30 minutes and the solid was collected. The final step of purification was performed by stirring the collected yellow solid in chloroform for a period of 30 minutes. The titled product was collected via filtration and dried in a desiccator. Yield 1.47 g, 67 %, $^1\text{H NMR}$ (CD_3OD , 400 MHz) δ_{H} 8.05 (m, 2H, *Ar o-CH*) 7.58 (m, 3H, *Ar p-CH*, *Ar m-CH*) $^{13}\text{C NMR}$ (CDCl_3 , 400 MHz) δ_{C} 131.9, 130.8, 130.6 FTIR (cm^{-1}) 3038 (aromatic C-H stretch) 1566, 1434, 733, 689 ES-MS 220 (M^+) 205, 204 ($\text{M} - \text{O}^2$) accurate mass spec: calculated mass 220.9463 formula: $\text{C}_6\text{H}_6\text{OI}$ m.p. 211 °C (decomposed).

General catalytic procedure (control reactions)

In a typical experiment 0.1 mmol of iodosylbenzene was added to a reaction vial, which was sealed and degassed thoroughly using low vacuum/ N_2 . A 2 mL solution of the solvent (dichloromethane/Dodecane) containing both 1 mmol cyclooctene substrate and 2.5 μmol porphyrin containing catalyst was then added via syringe. The suspension was then stirred in the dark for a period of thirty minutes under an atmosphere of nitrogen. After completion, the suspension was filtered using a Whatman[®] GD/X syringe filter, with a pore size of 0.45 μm , and transferred into a GC vial for analysis via manual injection.

General catalytic procedure – Colloidosome

In a typical experiment 0.1 mmol of iodosylbenzene was added to a reaction vial, which was sealed and degassed thoroughly using low vacuum/ N_2 . A colloidosome was synthesized by the homogenization of a 2 mL solution of the solvent (Dodecane) containing 1 mmol cyclooctene substrate, 8mg of PPG-TGI cross-linker and 2.5 μmol porphyrin containing catalyst and a 2 mL solution of the aqueous phase (1 % w/w aqueous solution of 125 nm PGMA₅₀-PS particles). Homogenization took place using an IKA Ultra-Turrax T-18 homogenizer with a 10 mm dispersing tool operating at 12 000 rpm for a period of 2 minutes. The colloidosome was injected into a reaction vial via a syringe and the suspension was then stirred in the dark for a period of thirty minutes under an atmosphere of nitrogen. After completion, the suspension was extracted using dichloromethane (5 mL) and the organic

layer was collected and filtered using a Whatman® GD/X syringe filter with a pore size of 0.45 µm. The filtrate was transferred into a GC vial for analysis via manual injection.

REFERENCES AND NOTES

1. (a) Immordino, M. L.; Dosio, F.; Cattel, L.; Stealth Liposomes: Review of The Basic Science, Rationale, and Clinical Applications, Existing and Potential. *Int J Nanomedicine*. **2006**, *1*(3): 297-315. (b) Muller, R. H.; Mader, K.; Gohla, S. Solid Lipid Nanoparticles (SLN) For Controlled Drug Delivery - A Review of the State of the Art. *Eur. J. of Pharm. and Biopharm.* **2000**, *50*, 161-77. (c) Hong; R.; Han, G.; Fernández, J. M.; Kim, B-J.; Forbes, N. S.; Rotello, V. M. Glutathione-Mediated Delivery and Release Using Monolayer Protected Nanoparticle Carriers *J. Am. Chem. Soc.*, **2006**, *128*(4), 1078-79.
2. (a) Yow, H. N.; Routh, A. F. Release Profiles of Encapsulated Actives from Colloidosomes Sintered for Various Durations. *Langmuir* **2009**, *25*, 159-66. (b) Gibbs, B. F.; Kermasha, S.; Alli, I.; Mulligan, C. N. Encapsulation in the Food Industry: a Review. *Int. J. Food Sci. Nutr.* **1999**, *50*(3), 213-24
3. Saraf, S.; Rathi, R.; Kaur, C. D.; Saraf, S. Colloidosomes an Advanced Vesicular System in Drug Delivery. *Asian J. Sci. Res.* **2011**, *4*(1), 1-15.
4. Pickering, S. U. Emulsions. *J. Chem. Soc., Trans.* **1907**, *91*, 2001-21.
5. (a) Li, M.; Harbron, R. L.; Weaver, J. V. M.; Binks, B. P.; Mann, S. Electrostatically Gated Membrane Permeability in Inorganic Protocells. *Nature Chem.* **2013**, *5*, 529-36. (b) Thompson, K. L.; Armes, S. P. From Well-Defined Macromonomers to Sterically-Stabilised Latexes to Covalently Cross-Linkable Colloidosomes: Exerting Control Over Multiple Length Scales. *Chem. Comm.* **2010**, *46*, 5274-76.
6. Dinsmore, A. D.; Hsu, M. F.; Nikolaidis, M. G.; Marquez, M.; Bausch, A. R.; Weitz, D. A. Colloidosomes: Selectively Permeable Capsules Composed of Colloidal Particles. *Science*. **2002**, *298*, 1006-9.
7. (a) Wu, C.; Bai, S.; Ansorge-Schumacher, M. B.; Wang, D. Nanoparticle Cages for Enzyme Catalysis in Organic Media. *Adv. Mater.* **2011**, *23*, 5694-99. (b) Buthe, A.; Kapitain, A.; Hartmeier, W.; Ansorge-Schumacher, M. B. Generation of Lipase-Containing Static Emulsions in Silicone Spheres for Synthesis in Organic Media. *J. Mol. Catal. B: Enzym.* **2005**, *35*, 93-99. (c) Wu, C.-Z.; Kraume, M.; Ansorge-

- Schumacher, M. B. Optimized Biocatalytically Active Static Emulsions for Organic Synthesis in Nonaqueous Media. *ChemCatChem* **2011**, *3*, 1314-19.
8. (a) K uchler, A.; Yoshimoto, M.; Luginb uhl, S.; Mavelli, F.; Walde, P. Enzymatic reactions in confined environments. *Nature Nanotech.* **2016**, *11*, 409. (b) Minten, I. J.; Claessen, V. I.; Blank, K.; Rowan, A. E.; Nolte, R. J. M.; J. L. M. Cornelissen, J. J. L. M. Catalytic Capsids: The Art of Confinement. *Chem. Sci.*, **2011**, *2*, 358-62.
 9. Keen, P. H. R.; Slater, N. K. H.; Routh, A. F. Encapsulation of Yeast Cells in Colloidosomes. *Langmuir* **2012**, *28*, 1169.
 10. Keen, P. H. R.; Slater, N. K. H.; Routh, A. F. Encapsulation of Lactic Acid Bacteria in Colloidosomes. *Langmuir* **2012**, *28*, 16007-14.
 11. Duan, H.; Wang, D.; Sobal, N. S.; Giersig, M.; Kurth, D. G.; Moehwald, H. Magnetic Colloidosomes Derived from Nanoparticle Interfacial Self-Assembly. *Nano Lett.* **2005**, *5*, 949-52.
 12. (a) Zheng, X.; Oviedo, I. R.; Twyman, L. J. Pseudo-Generational Effects Observed for a Series of Hyperbranched Polymers When Applied as Epoxidation Catalysts. *Macromolecules*, **2008**, *41*, 7776-79. (b) Ellis, A.; Twyman, L. J. Probing Dense Packed Limits of a Hyperbranched Polymer through Ligand Binding and Size Selective Catalysis.. *Macromolecules*. **2013**, *46*(17), 7055-7074.
 13. (a) Lindsey, J. S. Synthetic Routes to meso-Patterned Porphyrins. *Acc. Chem. Res.* **2010**, *43*, 300-11. (b) Geier, G. R., III; Ciringh, Y.; Li, F.; Haynes, D. M.; Lindsey, J. S. A Survey of Acid Catalysts for Use in Two-Step, One-Flask Syntheses of Meso-Substituted Porphyrinic Macrocycles. *Org. Lett.* **2000**, *2*, 1745-48. (c) Lindsey, J. S.; Wagner, R. W. *J. Org. Chem.* **1989**, *54*, 828.
 14. (a) Thompson, K. L.; Armes, S. P.; York, D. W.; Burdis, J. A. Synthesis of Sterically-Stabilized Latexes Using Well-Defined Poly(glycerol monomethacrylate) Macromonomers. *Macromolecules*, **2010**, *43*, 2169-77. (b) Thompson, K. L. PhD Thesis, Univesity of Sheffield, 2011
 15. (a) Thompson, K. L.; Armes, S. P.; Howse, J. R.; Ebbens, S.; Ahmad, I.; Zaidi, J. H.; York, D. W.; Burdis, J. A. Covalently cross-linked colloidosomes. *Macromolecules*, **2010**, *43*, 10466-74. (b) Mookhoek, S. D.; Blaiszik, B. J.; Fischer, H. R.; Sottos, N. R.; White, S. R.; van, d. Z. S. Peripherally Decorated Binary Microcapsules Containing Two Liquids. *J. Mater. Chem.* **2008**, *18*, 5390-94.
 16. This relatively low yield is due to the fact that dodecane is a non-polar solvent incapable of stabilizing the charged intermediates/transition states. Dodecane is also a

poor solvent for the oxygen source. To exclude the possibility that the oxygen source or porphyrin catalyst had degraded or was inactive, the reactivity was checked using a more suitable solvent (dichloromethane). After work up a yield of over 30% was obtained, which is typical of values we and others have previously obtained; see reference 12 above.

17. The reagents were not soluble in water, so the mixture was homogenized to maximize them “mixing” with polystyrene. Therefore, this control was a heterogeneous reaction that would likely proceed in low yield. Nevertheless, absolutely no product could be detected by GC. Although cyclooctene can be used as the core of a colloidosome, the amount of cyclooctene in our experiments was too small and a colloidosome did not form.
18. Although the product was not obtained in 100%, the small drop in yield can be accounted for by small losses during the extraction and analysis procedures.
19. Traylor, T. G.; Nakano, T.; Dunlap, B. E.; Traylor, P. S.; Dolphin, D. Mechanisms of hemin-catalyzed alkene epoxidation. The effect of catalyst on the regiochemistry of epoxidation. *J. Am. Chem. Soc.* **1986**, *108*, 2782-84.
20. Mecozzi, S.; West, A. P.; Dougherty, D. A; *Proc. Natl. Acad. Sci.*, **1996**, *93*, 10566.
21. Fendler, J. in *Catalysis in Micellar and Macromolecular Systems*, Academic Press, New York. 1995.
22. Ostovic, D.; Bruice, T. C. Intermediates in the Epoxidation of Alkenes by Cytochrome P-450 Models. 5. Epoxidation of Alkenes Catalyzed by a Sterically Hindered (Meso-Tetrakis(2,6-Dibromophenyl)Porphinato)Iron(III) Chloride. *J. Am. Chem. Soc.* **1989**, *111*, 6511-17.